Joint Electricity and Natural Gas Transmission Planning with Endogenous Market Feedbacks

Russell Bent, Seth Blumsack *Member, IEEE*, Pascal van Hentenryck *Member, IEEE*, Conrado Borraz-Sánchez, Mehdi Shahriari

***Abstract*—Recent trends in gas-fired power plant installation has increased the connections between the electric power and natural gas industries. Despite these dependencies, both industries must meet commercial, political, operational and technical requirements that often force the industries to plan and operate in isolation. As a result, undesired situations may arise, such as those experienced by both systems during the winter of 2013/2014 in the northeastern United States. In this paper, we consider the technical challenges and present a *Combined Electricity and Gas Expansion* (CEGE) planning model. The CEGE model minimizes the cost of meeting gas and electricity demand during high-stress conditions and introduces an elasticity model for analysis of gas-price volatility caused by congestion. The underlying mathematical formulation considers recent advances in convex approximations to make the problem computationally tractable when applied to large-scale CEGE instances. We conduct an in-depth analysis on integrated test systems that include the New England area.**

***Index Terms*—AC-OPF, Natural Gas, Convex Optimization, Second-Order Cone, Elasticity Model, Gas-Price Volatility, Heat-Rate Curves**

I. Introduction

As the price of natural gas has declined, power grids in many parts of North America have become increasingly reliant on natural gas as a fuel for the power generation fleet. This increasing dependence of the power grid on the supply system for a single fuel poses some risks, including gas supply vulnerabilities and gas price spikes caused by competition for scarce pipeline capacity and/or disruptions due to extreme weather conditions. Despite recent studies suggesting that large power grids could accommodate a substantial fraction of generation coming from natural gas during normal conditions [1], [2], extreme cold weather events during the winters of 2010/11 [3] and 2013/14 [4] have raised concerns among industry and regulators. Gas-fired power plants without on-site storage or dual-fuel capabilities may face fuel delivery insecurity arising from the interruptible nature of the gas transmission capacity contracts that many generators sign [4]. The asynchronous nature of gas and electric power price formation has also created uncertainty for gas-fired generators since they may receive commitment or dispatch instructions from the power grid operator without full knowledge of their marginal operating cost [5], [6].

Russell Bent is with T-Division: Applied Mathematics and Plasma Physics, Los Alamos National Laboratory, Los Alamos, NM, 87545 USA e-mail: rbent@lanl.gov

Seth Blumsack and Mehdi Shariari are with Pennsylvania State University, PA, USA.

Pascal van Hentenryck is with the University of Michigan, MI, USA.

Conrado Borraz-Sánchez is with Data& Analytics Lighthouse Center, KPMG LLP, Knoxville, TN 37919, email: cborrazsanchez@kpmg.com

In this paper, we introduce the Combined Electric and Gas Expansion (CEGE) planning model, an open-source optimization-based modeling framework that is computationally tractable for joint planning and operations problems involving interdependent natural gas and electric power transmission systems. The CEGE framework represents a contribution to a small, but growing, body of literature that considers joint expansion planning for natural gas and electric power transmission [7]–[18] in several distinct ways of interest to the power systems modeling and economics community. First, the CEGE model endogenizes price feedbacks from expansion decisions and incorporates these price feedbacks into the planning objective function. CEGE, to our knowledge, represents the first attempt to incorporate endogenously determined commodity prices into a joint gas-grid expansion planning model in a way that permits the joint optimization of capital and operational costs. It also identifies the tradeoffs involved in network hardening to avoid the economic consequences of weather events like the Polar Vortex that place coincident stress on both the gas and electricity networks.

Second, we demonstrate that the CEGE framework is computationally tractable for moderately sized joint gas-grid networks, despite the fact that it captures nonlinearities and does not rely on transportation flow or other linear approximations which were used in [8]–[10], [12], [19]–[23]. It thus builds on prior work focused on joint operational modeling of natural gas and electric power transmission systems [6], [19]–[26].

Third, we implement the CEGE framework on an integrated gas-grid test system with realistic topology. This test system is composed of the IEEE 36-bus NPCC electric power system [27] with marginal costs for coal, nuclear, hydro, wind, oil and refuse generation as reported in [28] and a multi-company gas transmission network covering the Pennsylvania-To-Northeast New England area in the US. This test system has been previously described in [16] but the present paper represents the first successful implementation of any planning or operational analysis on this benchmark. The value of this implementation to the research community is to provide the first set of public-domain performance benchmarks for joint gas-grid optimization problems that can be used in future research on improved algorithms or other modeling innovations.

Fourth, and perhaps most important for the research community, the CEGE model represents the first public-domain package that is able to handle joint gas-grid planning and operations problems on test systems with realistic topology. The modeling framework and test system data are available for use by any researcher. A very preliminary version of the CEGE framework was described in [16] but did not contain

the economic modeling features described in the present paper and was not tractably implemented on our Northeastern gas-grid test system.

By way of documenting the structure of CEGE package for the archival literature and illustrating some ways in which the modeling framework may be used (with computational performance benchmarks), we simulate three specific scenarios and compare the optimal investment plans arising from each. The first set of simulations solves for the lowest-cost investment plan to meet a specific level of demand for electricity and natural gas without considering the impacts of those investments on spot gas prices or power-plant fuel costs. For this "expansion only" set of scenarios, we find that substantial increases in demand are required to justify any additional network expansion. The second set of simulations solves the CEGE model for different levels of peak electricity and gas demand that vary spatially over our northeastern U.S. test system. These "endogenous price" simulations do consider the impacts of network expansions on gas prices, and we find that economic drivers would, in some cases, justify additional gas and electric transmission investments. We also simulate a scenario where the gas transmission network is hardened to an extent that would prevent large price spikes during extreme demand events. We find that the network investments required to avoid these price spikes would be substantial, around 40 percent higher than the cost of the investment plan that balances capital costs and network operational costs. Collectively, our results suggest that there is a strong economic justification for some level of coordinated infrastructure planning. However, a policy of expanding infrastructure solely to avoid extreme price spikes in electricity and gas markets is likely to be overly costly.

In Section II we provide a detailed specification of the CEGE model and discuss the relaxations that we implement in order for the CEGE framework to be computationally tractable. Section III describes the test system that we use to implement the CEGE framework, and provides specific information on how we endogenize commodity prices for natural gas in particular. The results of our computational experiments are described in Section IV, which includes a robustness check on the computational performance of the CEGE model to different natural gas price function specifications. We conclude in Section V with some thoughts on future directions for research on interdependent natural gas and electric power systems.

II. CEGE Optimization Problem

The CEGE optimization problem consists of constraints and variables associated with modeling the non-convex physics of electric power and natural gas systems, modeling expansion options and costs, modeling heat-rate curves, and incorporating power generation costs. Bold notation is used for constants, while underline and overline notation is used to denote lower and upper bounds. All edges in the model are undirected, so that a_{ij} refers to the arbitrary orientation of edge a from node i to node j. This convention is used when linking bus i to a. In this case, a_{ij} refers to those edges oriented from i to a node j and a_{ji} refers to those edges oriented from a node j to i.

Nomenclature

Electric Power Sets

N^e	set of electric power buses (nodes)
Ω	set of electric power generators
G_i	set of generators connected to bus i
N_i^e	set of buses connected to bus i by an edge
A^e	set of electric power lines (edges)

Electric Power Parameters

p_i^l, q_i^l	active and reactive load at bus i
gs_i, bs_i	active and reactive compensation at bus i
g_a, b_a, c_a	conductance, susceptance, and charging of edge a
r_a, Δ_a	tap ratio and phase shift of edge a
ξ_a	capacity rating of edge a
$\underline{p}_i^g, \overline{p}_i^g$	active power limits of generator i
$\underline{q}_i^g, \overline{q}_i^g$	reactive power limits of generator i
$\underline{v}_i, \overline{v}_i$	voltage magnitude limits of bus i
κ_a^e	cost of building edge a
$\mu_1^i, \mu_2^i, \mu_3^i$	production cost coefficients of generator i
ι	index of the reference bus
$\overline{\theta}$	maximum voltage angle difference between two buses connected by an edge

Electric Power Variables

p_{ij}	active power leaving bus i on an edge to bus j
q_{ij}	reactive power leaving bus i on an edge to bus j
p_j^g, q_j^g	active and reactive output of generator j
v_i, θ_i	voltage magnitude and phase angle at bus i
z_a^e	binary expansion variable for new edge a
w_i, w_{ia}	variable used for relaxing v_i^2 of bus i and relaxing v_i^2 of bus i with edge a
wr_a	variable used for relaxing $v_i v_j \cos(\theta_i - \theta_j)$ of edge a_{ij}
wi_a	variable used for relaxing $v_i v_j \sin(\theta_i - \theta_j)$ of edge a_{ij}

Natural Gas Sets

A_p^g	set of natural gas pipelines
A_c^g	set of natural gas compressors
A_v^g	set of natural gas valves
A^g	set of natural gas lines, $A_p^g \cup A_c^g \cup A_v^g$
N^g	set of natural gas junctions (nodes)

Natural Gas Parameters

w_a	resistance factor of pipeline a
$\hat{d}_i$	firm consumption at node i
$\underline{\alpha}_a, \overline{\alpha}_a$	(de)compression limits of edge a
$\underline{d}_i, \overline{d}_i$	limits on consumption at node i
$\underline{s}_i, \overline{s}_i$	limits on production at node i
$\underline{\pi}_i, \overline{\pi}_i$	limits on pressure squared at node i
z_a^g	binary expansion variable for new pipeline a
κ_a^g	cost of building pipeline a

Natural Gas Variables

π_i	pressure squared at node i
x_a	flow on edge a
s_i, d_i	flexible production and consumption at node i
y_a^+, y_a^-	binary direction variables for pipeline a
β_a	McCormick variables linking the pressure difference of pipeline a to flow direction

Coupling Sets

Γ_i	set of generators that consume gas at junction i
Z	set of pricing zones
N^g_ζ	set of junctions in zone ζ

Coupling Parameters

h^j_1, h^j_2, h^j_3	heat rate coefficients of generator j
$m^\zeta_1, m^\zeta_2, m^\zeta_3$	gas price coefficients in zone ζ
$n^\zeta_1, n^\zeta_2, n^\zeta_3$	gas pressure penalty coefficients in zone ζ
C_ζ	minimum cost of gas in zone ζ

Coupling Variables

ψ_ζ	cost of gas in zone ζ
γ_ζ	flexible gas consumed in zone ζ
ρ_ζ	maximum pressure squared in zone ζ
w_ζ	pressure penalty in zone ζ

A. Electric Power Model

The AC physics of electric power systems are governed by Kirchoff's and Ohm's laws. Within the CEGE, we use constraints

$$\textstyle\sum_{j\in G_i} p^g_j - \boldsymbol{p}^l_i - \boldsymbol{gs}_i v_i^2 = \sum_{j\in N^e_i} p_{ij} \quad \forall i \in N^e, \quad (1)$$

$$\textstyle\sum_{j\in G_i} q^g_j - \boldsymbol{q}^l_i + \boldsymbol{bs}_i v_i^2 = \sum_{j\in N^e_i} q_{ij} \quad \forall i \in N^e, \quad (2)$$

to model Kirchoff's laws. Here, N^e, G_i, and N^e_i model the sets of all buses (nodes), the generators connected to bus i, and the buses connected to bus i by an edge, respectively. Variables p_{ij} and q_{ij} model the active and reactive power leaving bus i on an edge to bus j respectively. Variables p^g_j and q^g_j model the active and reactive outputs of generator j. The notation v_i is used to denote the voltage magnitude of bus i. Finally, $\boldsymbol{p}^l_i$, $\boldsymbol{q}^l_i$, $\boldsymbol{gs}_i$, and $\boldsymbol{bs}_i$ are used to denote active load, reactive load, active compensation, and reactive compensation. The lossy Ohm's law is then modeled with these constraints $\forall a = a_{ij} \in A^e$

$$\begin{aligned} p_{ij} = {} & \tfrac{\boldsymbol{g}_a}{\boldsymbol{r}_a^2+\boldsymbol{\Delta}_a^2} v_i^2 - \tfrac{(\boldsymbol{g}_a\boldsymbol{r}_a+\boldsymbol{b}_a\boldsymbol{\Delta}_a)}{\boldsymbol{r}_a^2+\boldsymbol{\Delta}_a^2} v_i v_j \cos(\theta_i-\theta_j) \\ & - \tfrac{\boldsymbol{b}_a\boldsymbol{r}_a-\boldsymbol{g}_a\boldsymbol{\Delta}_a}{\boldsymbol{r}_a^2+\boldsymbol{\Delta}_a^2} v_i v_j \sin(\theta_i-\theta_j), \quad (3) \\ p_{ji} = {} & \boldsymbol{g}_a v_j^2 - \tfrac{(\boldsymbol{g}_a\boldsymbol{r}_a-\boldsymbol{b}_a\boldsymbol{\Delta}_a)}{\boldsymbol{r}_a^2+\boldsymbol{\Delta}_a^2} v_i v_j \cos(\theta_j-\theta_i) \\ & - \tfrac{\boldsymbol{b}_a\boldsymbol{r}_a+\boldsymbol{g}_a\boldsymbol{\Delta}_a}{\boldsymbol{r}_a^2+\boldsymbol{\Delta}_a^2} v_i v_j \sin(\theta_j-\theta_i), \quad (4) \\ q_{ij} = {} & -\tfrac{\boldsymbol{b}_a+\frac{\boldsymbol{c}_a}{2}}{\boldsymbol{r}_a^2+\boldsymbol{\Delta}_a^2} v_i^2 + \tfrac{\boldsymbol{b}_a\boldsymbol{r}_a+\boldsymbol{g}_a\boldsymbol{\Delta}_a}{\boldsymbol{r}_a^2+\boldsymbol{\Delta}_a^2} v_i v_j \cos(\theta_i-\theta_j) \\ & - \tfrac{\boldsymbol{g}_a\boldsymbol{r}_a+\boldsymbol{b}_a\boldsymbol{\Delta}_a}{\boldsymbol{r}_a^2+\boldsymbol{\Delta}_a^2} v_i v_j \sin(\theta_i-\theta_j), \quad (5) \\ q_{ji} = {} & (-\boldsymbol{b}_a + \tfrac{\boldsymbol{c}_a}{2}) v_j^2 + \tfrac{\boldsymbol{b}_a\boldsymbol{r}_a-\boldsymbol{g}_a\boldsymbol{\Delta}_a}{\boldsymbol{r}_a^2+\boldsymbol{\Delta}_a^2} v_i v_j \cos(\theta_j-\theta_i) \\ & - \tfrac{\boldsymbol{g}_a\boldsymbol{r}_a-\boldsymbol{b}_a\boldsymbol{\Delta}_a}{\boldsymbol{r}_a^2+\boldsymbol{\Delta}_a^2} v_i v_j \sin(\theta_j-\theta_i), \quad (6) \end{aligned}$$

The notation $\boldsymbol{g}_a$, $\boldsymbol{b}_a$, and $\boldsymbol{c}_a$ are used to denote the line conductance, susceptance, and charging respectively. Parameters $\boldsymbol{r}_a$ and $\boldsymbol{\Delta}_a$ are then used to model the transformer tap ratio and transformer phase shift. These are set to 1 and 0 respectively, for non-transformer lines. The notation θ_i is used to denote the voltage phase angle at bus i. The thermal limits and voltage phase angle difference of the lines are modeled using constraints

$$p_{ij}^2 + q_{ij}^2 \le \boldsymbol{\xi}_a^2, \quad \forall a = a_{ij} \in A^e, \quad (7)$$

$$p_{ji}^2 + q_{ji}^2 \le \boldsymbol{\xi}_a^2, \quad \forall a = a_{ij} \in A^e, \quad (8)$$

$$-\overline{\boldsymbol{\theta}} \le \theta_i - \theta_j \le \overline{\boldsymbol{\theta}}, \quad \forall a = a_{ij} \in A^e, \quad (9)$$

where $\boldsymbol{\xi}_a$ is the rating of the line. Finally, we bound voltage magnitudes, generator output, and reference bus phase angle with these constraints

$$\underline{\boldsymbol{p}}^g_i \le p^g_i \le \overline{\boldsymbol{p}}^g_i, \quad \forall i \in \Omega, \quad (10)$$

$$\underline{\boldsymbol{q}}^g_i \le q^g_i \le \overline{\boldsymbol{q}}^g_i, \quad \forall i \in \Omega, \quad (11)$$

$$\underline{\boldsymbol{v}}_i \le v_i \le \overline{\boldsymbol{v}}_i, \quad \forall i \in N^e, \quad (12)$$

$$\theta_\iota = 0 \quad (13)$$

where Ω denotes the set of all generators.

Expansion variables for new power lines are denoted with z^e_a. These variables are used to set q_{ij} and p_{ij} to 0 and these variables turn off Constraints (3)-(6) when $z^e_a = 0$. For example, Equation (3) becomes

$$p_{ij} = z^e_a(\cdot), \ \forall a = a_{ij} \in A^e, \quad (14)$$

where $(\cdot)$ is used to denote the right-hand side of Equation (3).

B. Natural Gas Model

The steady-state physics of natural gas systems are modeled using the Weymouth equations, which relate the flow of gas to pressure differences using the constraint

$$(\pi_i - \pi_j) = \boldsymbol{w}_a |x_a| x_a, \quad \forall a = a_{ij} \in A^g_p, \quad (15)$$

where A^g_p denotes the set of pipelines in the natural gas system. Here, π_i is used to denote the pressure squared at natural gas junction (node) i, $\boldsymbol{w}_a$ is the resistance factor of the pipe, and x_a is the flow of gas in the pipe. The Weymouth equations are a steady-state abstraction of the differential equations modeling gas flow in a pipe. They have been particularly effective in gas expansion planning (e.g., [29]). Like [29], we reformulate Eq. (15) with its disjunctive form, i.e.,

$$y^-_a U \le x_a \le y^+_a U, \quad (16)$$

$$y^-_a \underline{\boldsymbol{\pi}}_i \le \pi_i - \pi_j \le y^+_a \overline{\boldsymbol{\pi}}_i, \quad (17)$$

$$y^+_a + y^-_a = 1, \quad (18)$$

$$\beta_a \ge \pi_j - \pi_i + (\underline{\boldsymbol{\pi}}_i - \overline{\boldsymbol{\pi}}_j)(y^+_a + y^-_a + 1), \quad (19)$$

$$\beta_a \ge \pi_i - \pi_j + (\overline{\boldsymbol{\pi}}_i - \underline{\boldsymbol{\pi}}_j)(y^+_a + y^-_a - 1), \quad (20)$$

$$\beta_a \le \pi_j - \pi_i + (\overline{\boldsymbol{\pi}}_i - \underline{\boldsymbol{\pi}}_j)(y^+_a + y^-_a + 1), \quad (21)$$

$$\beta_a \le \pi_i - \pi_j + (\underline{\boldsymbol{\pi}}_i - \overline{\boldsymbol{\pi}}_j)(y^+_a + y^-_a - 1), \quad (22)$$

$$\beta_a = \boldsymbol{w}_a x_a^2, \quad (23)$$

for all $a = a_{ij}$, where $U = \sum_{i\in N^g} \overline{\boldsymbol{s}}_i$. Here Eqs. (16)-(18) force flow and pressure drops to match the direction of the pipe. Eqs. (19)-(22) linearize the absolute value of pressure drop, $\beta_a = (y^+_a - y^-_a)(\pi_i - \pi_j)$, using the standard McCormick

relaxation [30]. This linearization is exact because y_a^+ and y_a^- are binary. Eq. (23) restates the Weymouth equation using this disjunctive form.

Flow balance at the junctions is preserved using constraints

$$\sum_{a=a_{ij}\in A^g} x_a - \sum_{a=a_{ji}\in A^g} x_a = s_i - d_i - \hat{\boldsymbol{d}}_i, \quad \forall i \in N^g, \quad (24)$$

where A^g denotes all edges in the gas system. The notation s_i, d_i, and $\hat{\boldsymbol{d}}_i$ is used to model gas production, flexible gas consumption, and firm gas consumption respectively. N^g is used to refer to all junctions in the gas network. The change in pressure through compressors and control valves are modeled with constraints ($\forall a = a_{ij} \in A_c^g \cup A_v^g$,)

$$\pi_i \underline{\boldsymbol{\alpha}}_a - y_a^-(\overline{\boldsymbol{\pi}}_i \underline{\boldsymbol{\alpha}}_a - \underline{\boldsymbol{\pi}}_j) \le \pi_j \le \pi_i \overline{\boldsymbol{\alpha}}_a + y_a^-(\overline{\boldsymbol{\pi}}_j - \underline{\boldsymbol{\pi}}_i \overline{\boldsymbol{\alpha}}_a) \quad (25)$$

$$\pi_j \underline{\boldsymbol{\alpha}}_a - y_a^+(\overline{\boldsymbol{\pi}}_j \underline{\boldsymbol{\alpha}}_a - \underline{\boldsymbol{\pi}}_i) \le \pi_i \le \pi_j \overline{\boldsymbol{\alpha}}_a + y_a^+(\overline{\boldsymbol{\pi}}_i - \underline{\boldsymbol{\pi}}_j \overline{\boldsymbol{\alpha}}_a) \quad (26)$$

where $\underline{\boldsymbol{\alpha}_a}$ and $\overline{\boldsymbol{\alpha}_a}$ are used to denote the lower and upper (de)compression ratios (squared). For compressors (the set A_c^g), these values are typically ≥ 1 and for control valves (the set A_v^g) these values are typically ≤ 1. Control valves also include on/off variables to turn off these constraints and set $x = 0$ (see [29]). Finally, flexible consumption, production, and pressures are bound by the following constraints

$$\underline{\boldsymbol{d}}_i \le d_i \le \overline{\boldsymbol{d}}_i, \quad \forall i \in N^g, \quad (27)$$

$$\underline{\boldsymbol{s}}_i \le s_i \le \overline{\boldsymbol{s}}_i, \quad \forall i \in N^g, \quad (28)$$

$$\underline{\boldsymbol{\pi}}_i \le \pi_i \le \overline{\boldsymbol{\pi}}_i, \quad \forall i \in N^g, \quad (29)$$

Expansion variables for new natural gas pipelines are denoted with z_a^g. These variables are used to set x_a to 0 and turn off constraints (15) when $z_a^g = 0$, i.e.,

$$z_a^g \beta_a = \boldsymbol{w}_a x_a^2, \quad \forall a = a_{ij} \in A_p^g, \quad (30)$$

C. Heat Rate Model

The electric power and natural gas systems are connected by constraints representing heat rate curves of gas generators:

$$d_i = \sum_{j\in\Gamma_i} (\boldsymbol{h}_1^j + \boldsymbol{h}_2^j p_j^g + \boldsymbol{h}_3^j (p_j^g)^2), \forall i \in N^g. \quad (31)$$

Here, $\boldsymbol{h}$ describes the heat rate coefficients of a quadratic curve and Γ_i refers to those generators that consume gas at junction i. In the model, we use $\boldsymbol{h}_3 = 0$, so the constraint is convex. However, when $\boldsymbol{h}_3 \neq 0$, this is a non-convex constraint. Convexity is restored by relaxing equality to $\geq$. This relaxation allows solutions that consume more gas than the generator needs. Since the objective function (discussed later) penalizes congestion, this relaxation is generally tight. However, if it is beneficial to consume more gas, i.e., to lower pressure, then solutions will not be tight.

D. Endogenous Gas Price Determination

One of the key contributions of this paper is the endogenous modeling of natural gas prices, which will change based on construction of new natural gas pipelines or increased gas demand. We refer to this modeling approach as *endogenizing natural gas prices* because the prevailing gas price is determined by the chosen set of expansions, which in turn are chosen, in part, based on their impacts on the natural gas price. For a pricing zone, $\zeta \in Z$, there is a function $\mathcal{Z}(\zeta)$ that computes the location-specific natural gas price. From a pratical standpoint, as long as $\mathcal{Z}(\zeta)$ is convex, the addition of this term to the CEGE problem does not impact its overall computational complexity. We demonstrate this numerically in Section IV through the use of multiple convex parameterizations of $\mathcal{Z}(\zeta)$. Moreover, the definition of pricing zones can be as granular as desired. Our formulation of $\mathcal{Z}(\zeta)$ admits nodal pricing through the definition of a pricing function for each node, or zonal pricing by using a single pricing function for multiple nodes. In our simulation results in Section IV, we define two pricing zones for the purposes of illustration, but the modeling framework itself is highly flexible. The parameterization that we use in our simulations is described further in Section III.

E. Objective Function

The objective function of the CEGE defines the cost of expansion (building pipes and power lines), the cost of gas used by power generators, the cost to produce power for all non-gas fired generators, and the pressure penalty cost, i.e.,

$$\min \quad \sum_{a\in A^e} \boldsymbol{\kappa}_a^e z_a^e + \sum_{a\in A_p^g} \boldsymbol{\kappa}_a^g z_a^g + \sum_{\zeta\in Z} \mathcal{Z}(\zeta) + \sum_{i\in\Gamma} \boldsymbol{\mu}_1^i + \boldsymbol{\mu}_2^i p_i^g + \boldsymbol{\mu}_3^i (p_i^g)^2 \quad (32)$$

where $\boldsymbol{\kappa}^e$ and $\boldsymbol{\kappa}^g$ are used to denote the cost of building power lines and pipelines respectively, Γ refers to all generators in the model, and the coefficients $\boldsymbol{\mu}$ are used to quadratically cost power production. Since gas is already priced with ψ_ζ, $\boldsymbol{\mu}$ is typically 0 for all gas-fired generators. Also note that $\boldsymbol{\kappa} = 0$ and $z = 1$ for all existing pipes and power lines in the network.

F. MISOCP Relaxation

Given the complexity associated with solving this non-convex optimization problem, we reformulate the constraints associated with the Electric Power Model using the second-order cone (SOCP) relaxation discussed in [31]. Similarly, we reformulate the Natural Gas Model using the second order cone relaxation introduced in [29].

In the electric power model, the inclusion of the v_i^2, $v_i v_j \cos(\theta_i - \theta_j)$, and $v_i v_j \sin(\theta_i - \theta_j)$ terms yields non-convexities. The SOCP relaxation replaces these terms with lifted variables w_i, wr_a, and wi_a, respectively. Moreover, in order to model the on/off constraints for line flows, we also add a variable w_{ia}, where $w_{ia} = w_i$ when the line is built. These variables are bounded by

$$\underline{\boldsymbol{v}}_i^2 \le w_i \le \overline{\boldsymbol{v}}_i^2, \qquad \forall i \in N^e, \quad (33)$$
$$z_a \underline{\boldsymbol{v}}_i^2 \le w_{ia} \le z_a \overline{\boldsymbol{v}}_i^2, \qquad \forall a = a_{ij} \in A^e, \quad (34)$$
$$z_a \underline{\boldsymbol{v}}_j^2 \le w_{ja} \le z_a \overline{\boldsymbol{v}}_j^2, \qquad \forall a = a_{ij} \in A^e, \quad (35)$$
$$z_a \underline{\boldsymbol{v}}_i \underline{\boldsymbol{v}}_j \cos(\overline{\boldsymbol{\theta}}) \le wr_a \le z_a \overline{\boldsymbol{v}}_i \overline{\boldsymbol{v}}_j, \qquad \forall a = a_{ij} \in A^e, \quad (36)$$
$$z_a \overline{\boldsymbol{v}}_i \overline{\boldsymbol{v}}_j \sin(-\overline{\boldsymbol{\theta}}) \le wi_a \le z_a \overline{\boldsymbol{v}}_i \overline{\boldsymbol{v}}_j \sin(\overline{\boldsymbol{\theta}}), \quad \forall a = a_{ij} \in A^e, \quad (37)$$

The relationship between w_{ia} and w_i is formalized with

$$w_i - \overline{\boldsymbol{v}}_i^2(1 - z_a) \le w_{ia} \le w_i - \underline{\boldsymbol{v}}_i^2(1 - z_a), \quad (38)$$
$$w_j - \overline{\boldsymbol{v}}_j^2(1 - z_a) \le w_{ja} \le w_j - \underline{\boldsymbol{v}}_j^2(1 - z_a), \quad (39)$$

$\forall a = a_{ij} \in E^a$. Given that v and θ represent a complex number, w, wr, and wi are linked through

$$wi_a^2 + wr_a^2 \le w_i w_j, \quad (40)$$
$$wi_a^2 + wr_a^2 \le \overline{\boldsymbol{v}}_i^2 w_j z_a, \quad (41)$$
$$wi_a^2 + wr_a^2 \le w_i \overline{\boldsymbol{v}}_j^2 z_a, \quad (42)$$

for all $a = a_{ij} \in A^e$. Under this formulation, the voltage magnitudes (v) and voltage phase angles (θ) are implicit and constraints (9) are replaced with

$$\tan(-\overline{\boldsymbol{\theta}}) wr_a \le wi_a \le \tan(\overline{\boldsymbol{\theta}}) wr_a \quad \forall a \in E^a. \quad (43)$$

Eqs. (3)-(6) are then replaced with,

$$p_{ij} = \tfrac{\boldsymbol{g}_a}{\boldsymbol{r}_a^2 + \boldsymbol{\Delta}_a^2} w_{ia} - \tfrac{(\boldsymbol{g}_a \boldsymbol{r}_a + \boldsymbol{b}_a \boldsymbol{\Delta}_a)}{\boldsymbol{r}_a^2 + \boldsymbol{\Delta}_a^2} wr_a - \tfrac{\boldsymbol{b}_a \boldsymbol{r}_a - \boldsymbol{g}_a \boldsymbol{\Delta}_a}{\boldsymbol{r}_a^2 + \boldsymbol{\Delta}_a^2} wi_a \quad (44)$$
$$p_{ji} = \boldsymbol{g}_a w_{ja} - \tfrac{(\boldsymbol{g}_a \boldsymbol{r}_a - \boldsymbol{b}_a \boldsymbol{\Delta}_a)}{\boldsymbol{r}_a^2 + \boldsymbol{\Delta}_a^2} wr_a - \tfrac{\boldsymbol{b}_a \boldsymbol{r}_a + \boldsymbol{g}_a \boldsymbol{\Delta}_a}{\boldsymbol{r}_a^2 + \boldsymbol{\Delta}_a^2} wi_a \quad (45)$$
$$q_{ij} = -\tfrac{\boldsymbol{b}_a + \frac{\boldsymbol{c}_a}{2}}{\boldsymbol{r}_a^2 + \boldsymbol{\Delta}_a^2} w_{ia} + \tfrac{\boldsymbol{b}_a \boldsymbol{r}_a + \boldsymbol{g}_a \boldsymbol{\Delta}_a}{\boldsymbol{r}_a^2 + \boldsymbol{\Delta}_a^2} wr_a - \tfrac{\boldsymbol{g}_a \boldsymbol{r}_a + \boldsymbol{b}_a \boldsymbol{\Delta}_a}{\boldsymbol{r}_a^2 + \boldsymbol{\Delta}_a^2} wi_a \quad (46)$$
$$q_{ji} = (-\boldsymbol{b}_a + \tfrac{\boldsymbol{c}_a}{2}) w_{ja} + \tfrac{\boldsymbol{b}_a \boldsymbol{r}_a - \boldsymbol{g}_a \boldsymbol{\Delta}_a}{\boldsymbol{r}_a^2 + \boldsymbol{\Delta}_a^2} wr_a - \tfrac{\boldsymbol{g}_a \boldsymbol{r}_a - \boldsymbol{b}_a \boldsymbol{\Delta}_a}{\boldsymbol{r}_a^2 + \boldsymbol{\Delta}_a^2} wi_a \quad (47)$$

for all $a = a_{ij} \in A$. The only non-convexities of the gas model are in Eq (30). This is relaxed to the rotated second order cone constraint of the form

$$z_a^g \beta_a \ge \boldsymbol{w}_a x_a^2, \quad \forall a = a_{ij} \in A_p^g, \quad (48)$$

The implementation of these models is available for download at https://github.com/lanl-ansi/GasGridModels.jl.

G. Solution Approach

Within the expansion planning literature, most approaches and papers have focused on developing methods for optimizing the expansions with respect to approximations (i.e., the DC formulation of power systems) or relaxations, such as [32]. There is comparatively limited work on evaluating the quality of such solutions with respect to the full AC power flow physics. Here, we develop a procedure for finding a feasible solution based on a solution obtained using a relaxation or approximation. It is based on recently developed approaches for optimal power flow [31] that use the relaxed solution as an initial solution for gradient methods to find a locally optimal solution in the non-convex space. For this problem, we modify the approach by fixing the binary variables to the values found by the relaxation and then proceeding with the gradient method. Such a procedure (or something similar) is an important best practice for future work in expansion planning.

Algorithm 1 CEGE Solution Method

1: **function** SOLVECEGE($\mathcal{M}$)
2: $\quad \underline{\sigma} \leftarrow$ SOLVEMISCOP($\mathcal{M}$)
3: $\quad \overline{\sigma} \leftarrow$ SOLVENLP($\mathcal{M}, \underline{\sigma}$)
4: **return** $\langle \underline{\sigma}, \overline{\sigma} \rangle$
5: **end function**

This solution approach is outlined in pseudo code in Algorithm 1. Line 2 in Algorithm 1 solves the CEGE problem according to the MISOCP relaxation introduced earlier. The solution to the MISOCP is returned as a lower bound solution, $\underline{\sigma}$. Line 3 uses $\underline{\sigma}$ to recover a feasible solution to the original MINLP formulation. In the MINLP formulation, we replace all the binary variables with constants based on the assignments of those variables in the relaxed solution in $\underline{\sigma}$. The resulting problem is a non-linear program (NLP) that we solve to local optimality using a nonlinear solver (function SOLVENLP) to return an upper bound solution $\overline{\sigma}$. To improve convergence, SOLVENLP also imposes a constraint that states that the objective function needs to be within 5% of the objective value of $\underline{\sigma}$. This type of a constraint was also used in [33] in the context of AC optimal power flow to improve convergence. Line 4 returns the upper and lower bound solutions to the CEGE. While this approach is not guaranteed to find the globally optimal solution, as seen in Section IV, empirically, this approach yields good solutions with theoretically provable bounds on solution quality.

III. NORTHEASTERN UNITED STATES GAS GRID MODEL

We illustrate the tractability and utility of the CEGE using a new gas-grid test system, which is representative of the natural gas and electric power systems in the Northeastern United States. While the model has a realistic topology, it was constructed from multiple public sources and does not have the same level of detail as typically featured in electric power system planning cases. The data associated with this model are posted online at https://github.com/lanl-ansi/GasGridModels.jl.

a) Electric Power Model: The electric transmission system is based on the 36-bus NPCC model first discussed in [27]. Based on the bus names, we geo-located the buses to facilitate coupling the power system to the natural gas system. The original power system model has roughly 10% extra generation capacity. In order to stress electricity consumption in the NE model and focus our studies on the coupling between gas and power (and reflect the current trend to expand generation capacity with gas), we assume that there is infinite extra natural gas generation capacity at existing locations. Thus, the only constraints on satisfying increased demand for power arise from limitations in the natural gas and electric power transmission systems. Future work will include expansion models of generation.

Within the Northeastern United States, the mix of combined versus single cycle natural gas generation is not uniform. For example, the ratio of combined cycle plants to single cycle is much higher in New England than in New York. Locational differences in gas-fired power plant technology mix will naturally affect the costs of both gas and electricity prices. We built such technology variation into our test system by assigning each gas-fired generation node from [27] a share of combined and single cycle gas generation technology. These shares are based on EPA e-GRID data [34] for different utility service territories in the geographic footprint covered by our test system. Within this model, we included power line expansions in parallel with existing lines. Based on [35], the cost of new lines was set to $1.9M per mile for lines greater than 500 kV, $1.3M per mile for 345 kV lines, and $1M per miles for lines of 230 kV or smaller.

b) Natural Gas Model: The natural gas network for the Northeastern United States was constructed by using the gas delivery points described in [17]. We created firm gas demand profiles based on location-specific delivery data on the public posting web sites of natural gas transmission firms operating in the NE geographic area (a complete list of web sites was previously described in [17]). These firm gas demand profiles are assumed to be price-inelastic, and the only price-sensitive demand is assumed to be from electric power plants. Gas source points in our test system were identified by identifying marketing points (i.e., points of injection into the gas transmission system) in pipeline atlases published by the gas transmission firms operating in the NE region. We do not include gas storage facilities in our model, although the Leidy field in Northern Pennsylvania is represented in our model as a supply point. Gas storage is an important determinant of regional prices and supply, and will be included in a future version of the test system. The units of the flows are million standard cubic feet per day (Mmscfd). Pipelines between receipt points were built based on information in pipeline atlases posted on the public web sites of natural gas transmission companies. The resistance value of pipes was set using the function described in [36]

$$w_a = c * \frac{D_a^5 (2\log(\frac{3.6*D_a}{\epsilon}))^2}{zTL_a\Delta}, \quad \forall a \in A_p^g \tag{49}$$

where c is the gas relative constant (96.074830e-15), D is the diameter of the pipe in mm (we assume all pipes are 762 mm), ϵ is the absolute rugosity in mm (0.05), z is the gas compressibility factor (0.8), T is the gas temperature in K (281.15), Δ is the density of the gas relative to air (0.6106), and L is the pipe length in km (Euclidean distance). The system has 125 nodes and 143 (existing) edges.

In this model we assume that one pipe can be built in parallel with existing pipes and these parallel pipes have identical characteristics to existing pipes. The cost of building new pipes was set at $5M per mile [37].

c) Gas-Grid model: The natural gas generators of the electric power network were linked to the closest natural gas receipt point in the gas system. We used [38] to set the heat rate curve for single cycle gas generators to $h = [0, 0.48, 0]$ and to set the heat rate curve for combined cycle generators to $h = [0, 0.192, 0]$[1].

d) Endogenous gas pricing: To demonstrate endogenous gas price modeling, we develop a data driven gas pricing model based on the behavior of spot natural gas prices in the Northeastern U.S. in January 2014 (the month in which the Polar Vortex events occurred). Our implementation of the endogenous gas pricing model features two price zones based on Transco Zone 6 (Non New York) and the Transco Leidy Zone (extrapolated to include the other gas utilities in their region). We refer to these pricing zones as the cheap gas zone and the expensive gas zone to reflect the modeled difference in price sensitivity to network operating conditions. Based on analysis of historical price and operating data (Fig. 1), we parameterize the zonal pricing functions $\mathcal{Z}(\zeta)$ using quadratic functions. The pricing model links the price of gas to the total amount of gas consumption in a zone and includes a penalty cost on the maximum pressure in the zone. This builds on the intuition that consumption is linked to congestion through larger pressure differentials and the need to incur higher compression costs to deliver gas to constrained network locations. Spot gas prices will consequently rise in situations where demand is higher in a specific location, although this price sensitivity will vary by zone. We limit the penalty cost formulation to natural gas prices because those prices have historically been more volatile than prices for coal or nuclear fuel in the U.S., and oil is not a major component of the U.S. power generation fleet. The same type of formulation, however, could be used to endogenize the spot prices of other power-generation fuels where appropriate.

For a pricing zone, $\zeta \in Z$, where Z is the set of all zones (specifically, Transco Zone 6 and Transco Leidy Zone in our simulations), we calculate the cost of gas, ψ_ζ, with

$$\psi_\zeta \geq \boldsymbol{m}_1^\zeta + \boldsymbol{m}_2^\zeta \gamma_\zeta + \boldsymbol{m}_3^\zeta \gamma_\zeta^2, \tag{50}$$

where

$$\gamma_\zeta = \textstyle\sum_{i \in N_\zeta^g} d_i, \tag{51}$$

γ_ζ is the total amount of flexible gas consumed in ζ, and N_ζ^g are the junctions located in ζ. The coefficients, $\boldsymbol{m}$, are used to quadratically price the gas consumption. We calculated the pressure penalty cost based on the maximum pressure in ζ. The maximum pressure ρ_ζ is modeled with the constraints

$$\rho_\zeta \geq \pi_i, \forall i \in N_\zeta^g, \tag{52}$$

and the pressure penalty cost ω_ζ is calculated as

$$\omega_\zeta = \boldsymbol{n}_1^\zeta + \boldsymbol{n}_2^\zeta \rho_\zeta + \boldsymbol{n}_3^\zeta \rho_\zeta^2. \tag{53}$$

The coefficients $\boldsymbol{n}$ are used to quadratically price the pressure. This constraint is also not convex and we relax the equality with $\geq$. This relaxation is tight because ρ_ζ only influences a minimization term in the objective function.

[1]These numbers are based on converting Mmscfd into BTUs per MW/h

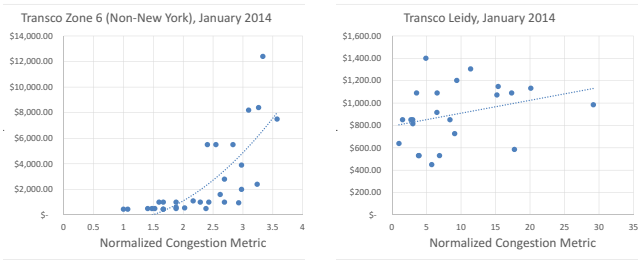

Fig. 1. Normalized price sensitivities for the expensive gas zone (left panel, based on Transco Zone 6 Non-New York) and the cheap gas zone (right panel, based on the Transco Leidy zone).

TABLE I
COEFFICIENTS USED IN DEMAND AND PRESSURE PRICING MODELS

Pressure Pricing

Transco Zone 6				Transco Leidy Zone			
Stress	n_1	n_2	n_3	Stress	n_1	n_2	n_3
-	0.0	-0.0064	2e-8	-	794.37	5e-5	0.0

Demand Pricing

Transco Zone 6				Transco Leidy Zone			
Stress	m_1	m_2	m_3	Stress	m_1	m_2	m_3
1.00	0.0	-4641.9	39.436	1.00	0.0	970.77	0.0161
2.25	0.0	-3714.3	47.446	2.25	0.0	980.97	0.0097
4.0	0.0	-1852.4	54.925	4.0	0.0	991.05	0.0033
6.25	0.0	1447.7	56.546	6.25	0.0	997.13	0.0007
9.0	0.0	5446.3	92.844	9.0	0.0	1001.9	0.0040

For this pricing model, we add a minimum price constraint of the form

$$\psi_\zeta \geq \boldsymbol{C}_\zeta \gamma_\zeta, \tag{54}$$

where $\boldsymbol{C}_\zeta$ denotes a linear coefficient on the minimum cost of gas. We impose this constraint to avoid model solutions with negative gas prices.Thus, for the purposes of this paper, $\mathcal{Z}(\zeta) = \psi_\zeta + \omega_\zeta$.

Implementation of the zonal pricing model used data on spot natural gas prices for the two areas obtained from the SNL Financial database, as well as operational data published on the Transco 1Line web site (http://www.1line.williams.com/Transco/index.html).

In Figure 1, we plot the prices in each zone as a function of normalized demand and we fit a convex quadratic polynomial to this data. The coefficients of this polynomial, shown in Table I, serve as the coefficients in the pressure penalty cost equation 53. There is thus a greater sensitivity of the spot gas price to pressure conditions in the expensive gas zone than in the cheap gas zone. We set $C = 450$ for the expensive gas zone and we set $C = 530$ for the cheap gas zone. We also put a minimum price of 0 for the pressure penalty pricing. For the expensive gas zone, the price curve is < 0 when the pressure is < 566, so any pressure below this has no penalty. The coefficients for demand-based pricing vary depending on the firm demand in the system, because we assume only flexible demand (i.e., gas power plants) is price-sensitive.

e) Network Stress: We generated variations of the NE Model to stress the system and analyze the impact of stress to the system design and overall gas prices. We uniformly stressed the power system by multiplying the power demand by a value in $\{1.0, 1.1, 1.25, 1.3, 1.35\}$. Similarly, we uniformly stressed the natural gas system by multiplying the firm gas demand by a value in $\{1.0, 2.25, 4.0, 6.25, 9.0\}$.

IV. NUMERICAL RESULTS

In this section, we describe the numerical results of applying the CEGE to the NE Model. The MISCOP of the CEGE model are solved using Gurobi 7.0.1. The NLP model is solved using Knitro 9.1.0. All computations were performed with an Intel(R) Xeon(R) CPU E5-2660 v3 processor (2.60 GHz) and 62 GB of memory.

A. Uniform Stress

We illustrate the capabilities of the model by increasing the consumption of gas at each gas demand node by a uniform proportion and increasing the consumption of electricity at each electricity demand node by a uniform proportion. For these stress cases, a 12 hour time limit was placed on computing solutions to the MISOCP relaxation of the CEGE. In order to obtain a more reasonable balance between expansion and operational costs, we multiplied the cost of operations by 365 in the CEGE objective function. This represents minimizing the combined expansion cost and operational cost for a full year, assuming uniform daily levels of demand. This assumption can be relaxed in future work to consider peak/off-peak demand scenarios for electricity and natural gas. The pressure penalty cost relative to the cost of gas consumption was adjusted so that these costs had roughly the same order of magnitude within each gas pricing zone. The pressure penalty of Zone 6 is multiplied by 175 and the pressure penalty of the Leidy zone is multiplied by 600.

Table II describes the quality of the solutions for different levels of uniform stress for the endogenous-price model and compares them with an alternative objective formulation (expansion-only) which excludes the operational cost terms. This allows us to isolate design choices made for feasibility from design choices made to improve the operating costs[2]. In Table II, the first column shows the multiplier applied to all fixed gas demand. The remainder of the table is divided into five groups, where each group shows results for the power demand specified in the first row. Within each group, the columns labeled Obj, Gap, and CPU report the objective value of the relaxed solution (TO is used to indicate time out), its optimality gap, and the CPU time required to solve the problem. The column labeled $\overline{\text{Obj}}$ reports the objective value of the primal feasible solution and the column labeled $\overline{\text{Gap}}$ reports the gap between the primal feasible solution and the relaxed solution. All objective values are scaled by 1.0E8. All gaps are reported in terms of percentages. Values with no % symbol report the relative feasibility error. Except in the most extreme gas stress cases (stress multiplier of 9.0), the CEGE problem is computationally tractable to solve. Generally speaking, the

[2]Objective values are not directly comparable as the operating costs for the expansion only solutions do not include the actual operating costs

TABLE II
THE CEGE SOLUTIONS FOR THE UNIFORMLY STRESSED NE MODEL. THE COLUMNS ARE USED TO STRESS THE POWER SYSTEM (PS). THE ROWS ARE USED TO STRESS THE GAS SYSTEM (GS).

Expansion-Only Model

	1.0 PS					1.1 PS					1.25 PS					1.3 PS					1.35 PS				
	$\underline{\text{Obj}}$	$\underline{\text{Gap}}$	$\underline{\text{CPU}}$	$\overline{\text{Obj}}$	$\overline{\text{Gap}}$	$\underline{\text{Obj}}$	$\underline{\text{Gap}}$	$\underline{\text{CPU}}$	$\overline{\text{Obj}}$	$\overline{\text{Gap}}$	$\underline{\text{Obj}}$	$\underline{\text{Gap}}$	$\underline{\text{CPU}}$	$\overline{\text{Obj}}$	$\overline{\text{Gap}}$	$\underline{\text{Obj}}$	$\underline{\text{Gap}}$	$\underline{\text{CPU}}$	$\overline{\text{Obj}}$	$\overline{\text{Gap}}$	$\underline{\text{Obj}}$	$\underline{\text{Gap}}$	$\underline{\text{CPU}}$	$\overline{\text{Obj}}$	$\overline{\text{Gap}}$
1.0 GS	0	0%	10	0	1e-3	0	0%	13	0	2e-3	0.58	0%	4	0.58	1e-4	0.58	0%	15	0.58	7e-4	7.82	0%	21	7.82	0%
2.25 GS	0	0%	58	0	1e-2	0	0%	31	0	3e-3	0.58	0%	9	0.58	0%	0.58	0%	25	0.58	3e-4	7.82	0%	30	7.82	3e-4
4.0 GS	0	0%	214	0	3e-3	0	0%	200	0	2e-3	0.58	0%	36	0.58	6e-4	0.58	0%	24	0.58	4e-3	7.82	0%	23	7.82	2e-3
6.25 GS	0	0%	1950	0	7e-3	0	0%	11790	0	6e-3	0.58	0%	156	0.58	5e-4	0.58	0%	67	0.58	3e-3	7.82	0%	56	7.82	2e-4
9.0 GS	2.74	100%	TO	2.74	3e-4	1.75	100%	TO	1.75	3e-4	2.81	79.2%	TO	2.81	2e-4	2.72	78%	TO	2.72	2e-4	10.6	23.7%	TO	10.6	5e-4

Endogenous-Price Model

	1.0 PS					1.1 PS					1.25 PS					1.3 PS					1.35 PS				
	$\underline{\text{Obj}}$	$\underline{\text{Gap}}$	$\underline{\text{CPU}}$	$\overline{\text{Obj}}$	$\overline{\text{Gap}}$	$\underline{\text{Obj}}$	$\underline{\text{Gap}}$	$\underline{\text{CPU}}$	$\overline{\text{Obj}}$	$\overline{\text{Gap}}$	$\underline{\text{Obj}}$	$\underline{\text{Gap}}$	$\underline{\text{CPU}}$	$\overline{\text{Obj}}$	$\overline{\text{Gap}}$	$\underline{\text{Obj}}$	$\underline{\text{Gap}}$	$\underline{\text{CPU}}$	$\overline{\text{Obj}}$	$\overline{\text{Gap}}$	$\underline{\text{Obj}}$	$\underline{\text{Gap}}$	$\underline{\text{CPU}}$	$\overline{\text{Obj}}$	$\overline{\text{Gap}}$
1.0 GS	40.3	0%	39	42.2	4.7%	49.3	0%	33	51.7	4.9%	63.7	0%	53	66.9	5.0%	70.2	0%	49	70.6	0.5%	82.2	0%	2908	82.2	0%
2.25 GS	41.9	0%	69	44.0	5.0%	51.3	0%	40	53.8	4e-6	66.3	0%	36	69.6	4.9%	72.9	0%	84	72.9	0%	85.4	0%	585	89.6	4.9%
4.0 GS	43.9	0%	484	43.9	0%	53.7	0%	640	53.7	0.0%	69.6	0%	443	69.6	0%	76.4	0%	368	80.2	4.9%	89.1	0%	1438	89.1	0%
6.25 GS	46.2	0%	11188	48.5	4.9%	56.4	0%	1666	59.2	4.9%	73.1	0%	20435	76.7	4.9%	80.2	0.5%	TO	84.2	6.8%	93.1	0.2%	TO	97.7	5.1%
9.0 GS	60.5	13.1%	TO	59.1	5e-2	72.4	11.2%	TO	76.1	18.3%	92.2	9.4%	TO	96.8	15.9%	100.8	9.2%	TO	100.8	9.2%	115	8.9%	TO	115	8.9%

TABLE III
DESIGN AND OPERATING PROPERTIES OF CEGE SOLUTIONS FOR THE UNIFORMLY STRESSED NE MODEL.

Expansion Model

	1.0 PS						1.1 PS						1.25 PS						1.3 PS						1.35 PS					
	z^e	z^g	γ_6	γ_L	$\sqrt{\rho_6}$	$\sqrt{\rho_L}$	z^e	z^g	γ_6	γ_L	$\sqrt{\rho_6}$	$\sqrt{\rho_L}$	z^e	z^g	γ_6	γ_L	$\sqrt{\rho_6}$	$\sqrt{\rho_L}$	z^e	z^g	γ_6	γ_L	$\sqrt{\rho_6}$	$\sqrt{\rho_L}$	z^e	z^g	γ_6	γ_L	$\sqrt{\rho_6}$	$\sqrt{\rho_L}$
1.0 GS	0	0	209	567	560	504	0	0	239	643	566	505	1	0	293	745	574	620	1	0	316	779	566	506	5	0	332	822	527	643
2.25 GS	0	0	209	567	531	506	0	0	239	643	566	507	1	0	290	745	619	640	1	0	302	779	823	785	5	0	334	822	593	800
4.0 GS	0	0	209	568	566	551	0	0	239	643	566	549	1	0	287	745	616	820	1	0	301	779	582	1032	5	0	317	822	621	957
6.25 GS	0	0	209	570	563	1153	0	0	239	646	642	1103	1	0	287	751	726	1116	1	0	298	795	903	1096	5	0	273	776	846	1117
9.0 GS	0	0	120	298	995	1159	0	5	160	370	1149	1200	1	5	174	548	1148	1200	1	6	210	437	1141	1200	5	7	285	517	995	1195

Endogenous-Price Model

	1.0 PS						1.1 PS						1.25 PS						1.3 PS						1.35 PS					
	z^e	z^g	γ_6	γ_L	$\sqrt{\rho_6}$	$\sqrt{\rho_L}$	z^e	z^g	γ_6	γ_L	$\sqrt{\rho_6}$	$\sqrt{\rho_L}$	z^e	z^g	γ_6	γ_L	$\sqrt{\rho_6}$	$\sqrt{\rho_L}$	z^e	z^g	γ_6	γ_L	$\sqrt{\rho_6}$	$\sqrt{\rho_L}$	z^e	z^g	γ_6	γ_L	$\sqrt{\rho_6}$	$\sqrt{\rho_L}$
1.0 GS	5	0	181	600	528	503	5	0	211	677	520	504	7	0	253	802	566	508	8	0	269	848	566	506	13	0	274	897	537	507
2.25 GS	5	0	181	600	558	535	8	0	196	693	566	558	8	0	247	810	566	535	10	0	253	865	566	515	13	0	268	897	565	508
4.0 GS	8	0	166	616	566	538	8	0	196	693	566	602	10	0	235	826	566	537	10	0	250	865	566	559	13	0	260	897	565	542
6.25 GS	7	0	162	616	573	1120	8	0	196	694	580	1145	10	0	235	827	606	1144	10	0	249	865	615	1144	13	0	260	897	623	1120
9.0 GS	8	14	158	621	736	1116	9	13	185	696	804	1134	11	14	225	831	845	1125	13	13	234	870	802	1080	16	12	249	902	842	1118

TABLE IV
COST PROPERTIES OF CEGE SOLUTIONS FOR THE UNIFORMLY STRESSED NE MODEL.

Expansion-Only Model

	1.0 PS				1.1 PS				1.25 PS				1.3 PS				1.35 PS			
	ζ_6	ζ_L	$\frac{\zeta_6}{\gamma_6}$	$\frac{\zeta_L}{\gamma_L}$	ζ_6	ζ_L	$\frac{\zeta_6}{\gamma_6}$	$\frac{\zeta_L}{\gamma_L}$	ζ_6	ζ_L	$\frac{\zeta_6}{\gamma_6}$	$\frac{\zeta_L}{\gamma_L}$	ζ_6	ζ_L	$\frac{\zeta_6}{\gamma_6}$	$\frac{\zeta_L}{\gamma_L}$	ζ_6	ζ_L	$\frac{\zeta_6}{\gamma_6}$	$\frac{\zeta_L}{\gamma_L}$
1.0 GS	0.7	1.0	0.4	0.2	1.1	1.1	0.5	0.2	2.0	1.2	0.7	0.2	2.5	1.3	0.8	0.2	2.8	1.3	0.8	0.2
2.25 GS	1.3	1.0	0.6	0.2	1.8	1.1	0.8	0.2	3.0	1.2	1.0	0.2	4.0	1.3	1.3	0.2	4.1	1.3	1.2	0.2
4.0 GS	2.0	1.0	1.0	0.2	2.7	1.1	1.1	0.2	4.1	1.2	1.4	0.2	4.5	1.3	1.5	0.2	5.1	1.3	1.6	0.2
6.25 GS	2.8	1.1	1.3	0.2	3.7	1.2	1.6	0.2	5.4	1.3	1.9	0.2	6.9	1.3	2.3	0.2	5.6	1.3	2.1	0.2
9.0 GS	4.3	0.8	3.6	0.3	7.9	0.9	4.9	0.2	8.3	1.1	4.8	0.2	9.7	1.0	4.6	0.2	13	1.3	4.6	0.2

Endogenous-Price Model

	1.0 PS				1.1 PS				1.25 PS				1.3 PS				1.35 PS			
	ζ_6	ζ_L	$\frac{\zeta_6}{\gamma_6}$	$\frac{\zeta_L}{\gamma_L}$	ζ_6	ζ_L	$\frac{\zeta_6}{\gamma_6}$	$\frac{\zeta_L}{\gamma_L}$	ζ_6	ζ_L	$\frac{\zeta_6}{\gamma_6}$	$\frac{\zeta_L}{\gamma_L}$	ζ_6	ζ_L	$\frac{\zeta_6}{\gamma_6}$	$\frac{\zeta_L}{\gamma_L}$	ζ_6	ζ_L	$\frac{\zeta_6}{\gamma_6}$	$\frac{\zeta_L}{\gamma_L}$
1.0 GS	0.4	1.1	0.3	0.2	0.8	1.2	0.4	0.2	1.3	1.3	0.5	0.2	1.6	1.3	0.6	0.2	1.7	1.4	0.6	0.2
2.25 GS	0.9	1.1	0.5	0.2	1.1	1.2	0.6	0.2	2.0	1.3	0.8	0.2	2.1	1.3	0.8	0.2	2.4	1.4	0.9	0.2
4.0 GS	1.2	1.1	0.7	0.2	1.7	1.2	0.9	0.2	2.6	1.3	1.1	0.2	3.0	1.4	1.2	0.2	3.2	1.4	1.3	0.2
6.25 GS	1.7	1.1	1.1	0.2	2.4	1.2	1.3	0.2	3.5	1.3	1.5	0.2	4.0	1.4	1.6	0.2	4.3	1.4	1.7	0.2
9.0 GS	3.7	1.1	2.3	0.2	5.0	1.2	2.7	0.2	7.0	1.4	3.1	0.2	7.1	1.4	3.0	0.2	8.1	1.4	3.3	0.2

design solutions based on the relaxation have feasible (albeit higher) operating costs. Even in those cases where a feasible solution is not found, the worst infeasibility is relatively small.

The design and operating choices for both methods (the expansion-only model and endogenous-price model considering both expansion and operational costs) are shown in Table III. This table is structured in the same way as Table II. Here, z^e refers to the number of power lines that were built; z^g refers to the number of pipe lines built; γ_6 and γ_L refer to the Mmscfd used in Zone 6 and Leidy Zone to produce power; ρ_6 and ρ_L refer to maximum pressure squared in the two zones. In the expansion only model, there are fewer expansions in both the natural gas and electric power transmission systems built for feasibility requirements (i.e., for reliability). Once the power system is stressed by a factor of 1.25 in the expansion-only model, one power line is built. Even at 1.35, only five power lines are built. Similarly, gas pipelines are only built in the 9.0 stress case. In contrast, the endogenous-price model encourages additional expansions to decrease operational costs. In the gas stress cases < 9.0, between $5-10$ additional power lines are added to the network. These choices are made to shift gas demand used to produce power from the high-cost gas zone in the eastern portion of our test system to the low-cost gas zone in the western portion of our test system. In this case, gas by wire is the cheaper option to deliver additional electricity to the constrained area of our network. This is in some contrast to prior work [39], which suggests that, in the presence of static prices, transportation of gas via pipeline is more cost-effective than moving gas by wire. The operating condition results for the gas stress 9.0 are even more interesting. Here, the maximum pressure in the high gas price zone for the expansion-only model is near the upper limit and incurs a very high penalty pressure cost[3]. In contrast, the endogenous-price model builds significantly more gas pipelines to drive those pressures down. These observations are reinforced by Table IV where the actual operating costs are shown. Here, the extra pipes and power lines are clearly used to drive the costs associated with Zone 6 down. In this table, $\zeta_i = \psi_i + \omega_i$ refers to the total daily amount of procured gas for generation in each price zone, scaled by 10^6, and $\frac{\zeta}{\gamma}$ tracks the daily price per Mmscfd, scaled by 10^4.

B. Avoiding Extreme Price Spikes

We also considered constraining the expansion problems so that the network expansions are sufficient to avoid extreme price spikes like those that arose during the polar vortex event during the winter of 2014. We impose a limit on the pressure penalty costs, which caps price spikes in constrained areas of the gas network. The network expansion problem determines how best to expand the network while staying within the prescribed limit. The results are described in Table V, where the limit is computed using the penalty obtained in the optimal solution of the CEGE problem presented earlier. In particular, the results present the network expansion when the limit is set to 100%, 10%, 5%, 1%, and 0% of the penalty for the 9.0 GS and 1.35 PS problem. The variables z^e, z^g, Obj and Gap have the same interpretation as in Tables II-IV. Interestingly, the gas network must be expanded by another 40% compared to earlier results to avoid the types of price spikes that were observed during the polar vortex, as soon as the penalty is limited to 10% or less. The electricity network is not affected in this case, consistent with the observation that gas transmission was scarce during the polar vortex, not gas supply *per se*. Our results do suggest that a policy of infrastructure hardening to avoid the economic consequences of weather-driven demand spikes in the electricity and natural gas systems would be costly, relative to the benefits of spot gas price reduction, and would need to be concentrated on enhancing fuel delivery rather than electric power delivery.

[3]As a post processing step, we minimized the operating costs for the expansion design to produce these results.

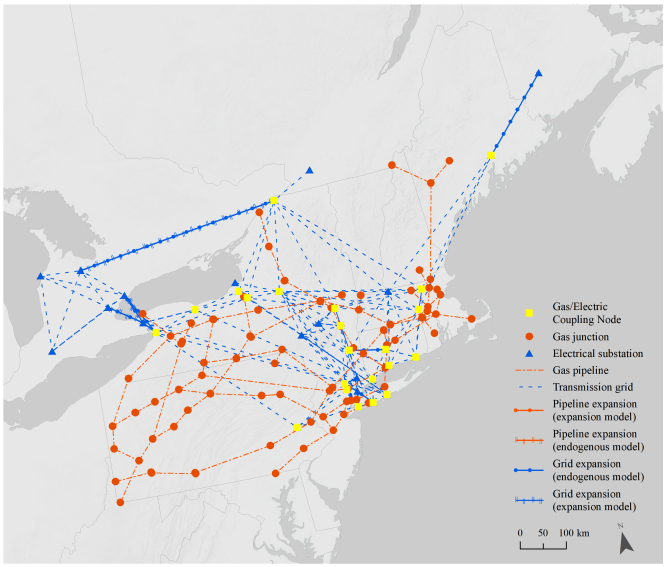

Fig. 2. Electric and gas transmission network additions in the 2.25 gas stress and 1.35 electric power stress case.

C. Non Uniform Stress

Finally, we consider a scenario where gas system stress is not uniform over space. The power system is stressed at the 1.35 level at every electricity consumption point in our test system. We increase the gas demand for customers other than power plants in the western portion of our test system (corresponding roughly to western Pennsylvania and New York) by a multiplicative factor of 13.0 (if $\hat{d} < 1$, we assume $\hat{d} = 1$ for the purposes of computing stress here), reflecting a type of scenario where gas demand in one portion of our network is driven by commercial or industrial applications and not by the power generation sector. The optimality gap of the convex relaxations for this non-uniform stress scenario is 0.16%. The outcome of this scenario is compared to the 1.35 power stress, 9.0 uniform natural gas stress scenario from Table III. Increasing the gas stress only in the western portion of our test system actually leads to a smaller number of gas pipelines being built as compared to a scenario where gas demand increases by a smaller amount uniformly throughout

TABLE V
PROPERTIES OF THE 9.0 GS PROBLEM WHEN THE PRESSURE PENALTY COST IS RESTRICTED TO AVOID EXTREME SPIKES IN NATURAL GAS PRICES.

	1.0 PS				1.1 PS				1.25 PS				1.3 PS				1.35 PS			
	z_e	z_p	Obj	Gap	z_e	z_p	Obj	Gap	z_e	z_p	Obj	Gap	z_e	z_p	Obj	Gap	z_e	z_p	Obj	Gap
100%	8	14	60.5	13.1%	9	13	73.2	11.8%	11	14	95.1	11.8%	13	13	100.8	9.2%	16	12	115	8.9%
10%	7	17	63.6	16.7%	10	15	75.4	12.3%	10	17	95.6	12.2%	11	17	104.6	12.0%	14	17	118	11.1%
5%	8	15	64.2	18.1%	10	14	76.8	16.1%	10	17	97.1	13.2%	10	19	105.9	12.8%	16	17	119	11.2%
1%	9	17	64.2	19.7%	9	19	77.5	16.3%	10	19	99.2	14.1%	10	19	106.4	11.9%	16	17	122	12.4%
0%	8	16	64.2	15.6%	10	17	77.5	13.6%	11	18	99.8	14.0%	11	20	107.9	12.1%	16	19	122	11.7%

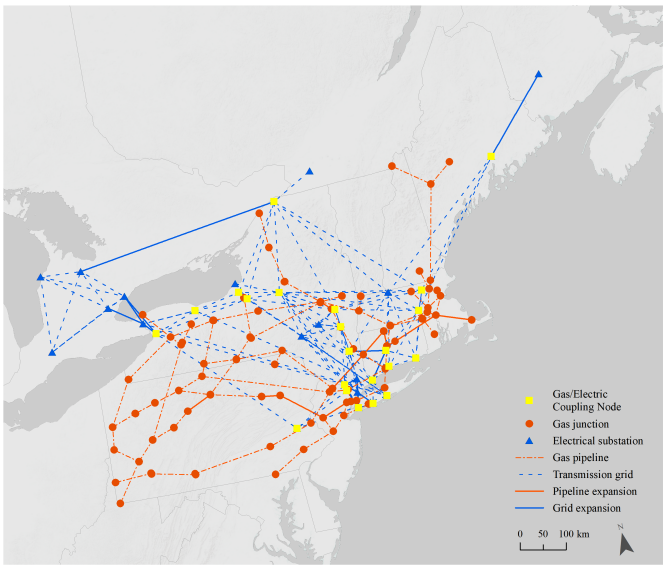

Fig. 3. Electric and gas transmission network additions in a scenario where gas stress is at the 9.0 level and uniformly distributed over space and electric stress is at the 1.35 level.

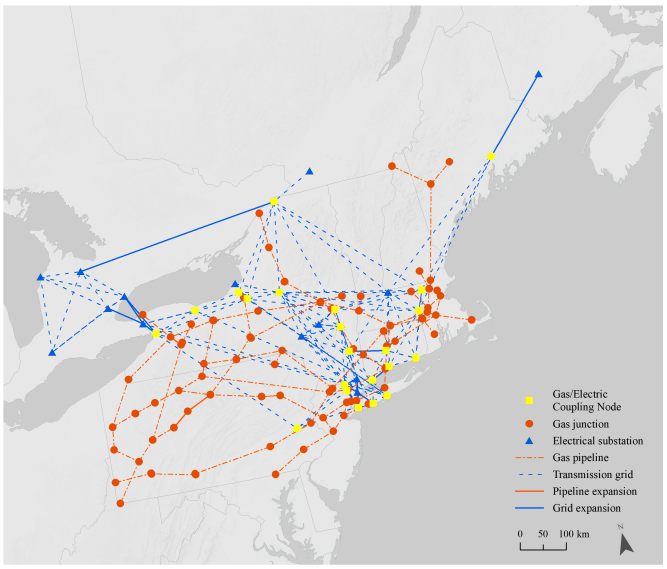

Fig. 4. Electric and gas transmission network additions in a scenario where gas stress is at the 13.0 level in the western portion of the test system and electric stress is at the 1.35 level, uniformly distributed over space.

the entire test system (16 pipelines in the case shown in Figure 3 versus 4 pipelines in the case shown in Figure 4).

D. Gas Transmission Expansion Options

In our simulations, we allow any existing gas or electric transmission corridor to expand its capacity and allow some new gas pipeline corridors to be added. The options for new candidate corridors are defined based on proposed gas pipeline expansions in the northeastern U.S. These expansions would all facilitate additional gas shipments from the Marcellus Shale producing area in Pennsylvania to demand centers in the Mid-Atlantic, New York, and New England. The specific expansions are listed below, with their geographic locations and names of the proposed pipeline expansions on which our modeled expansions are based.

1) NG1: A new east-west link across PA (expansion of the Texas East line)
2) NG2: A new link increasing delivery into eastern PA and NJ (the Penn East line)
3) NG3: New links from north-central PA to the south and northeast (the Transco expansions)
4) NG4: A new link from north-central PA going north towards NY (the Marc II line)
5) NG5: A new link from PA to NY (the Constitution line)
6) NG6: A new link increasing delivery from north-central PA to southeastern PA (the Sunbury line)

TABLE VI
NEW GAS TRANSMISSION CORRIDORS BUILT IN HIGH GAS STRESS CASES.

Power System Stress Case	New Gas Transmission
1.0 PS	NG3
1.1 PS	NG3 and NG6
1.25 PS	NG2 and NG6
1.3 PS	NG2 and NG6
1.35 PS	NG2 and NG6

In our simulations, new pipeline corridor expansions were chosen in the highest gas stress cases as lower-cost alternatives to expanding existing corridors to meet higher gas demand and to ameliorate gas price spikes. The new pipeline corridors that were chosen by the model did vary by the power system stress case, as shown in Table VI. At lower levels of power system stress, the model adds combinations of new gas corridors NG3 and NG6, which would expand gas deliveries from the Marcellus producing areas to areas of higher gas prices in New York and the Mid-Atlantic coast. At higher levels of power system stress, the model adds NG2 and NG6, which expand gas delivery capability into the Mid-Atlantic coastal areas rather than expanding capacity into New York.

TABLE VII
COST AND DESIGN PROPRIETIES OF THE CEGE SOLUTIONS FOR ALTERNATE ENDOGENOUS PRICING MODELS

	1.35 PS (Apr)				1.35 PS (Jul)				1.35 PS (Oct)			
	Obj	Gap	z^e	z^g	Obj	Gap	z^e	z^g	Obj	Gap	z^e	z^g
1.0 GS	72.0	0.0%	6	0	72.2	0.0%	6	0	72.0	0.0%	6	0
6.25 GS	72.2	0.0%	6	0	73.0	0.1%	6	0	72.0	0.0%	6	0
9.0 GS	76.3	6.1%	6	10	79.0	5.2%	6	10	75.8	5.1%	6	10

TABLE VIII
COEFFICIENTS USED IN DEMAND AND PRESSURE PRICING MODELS FOR THE ALTERNATE PRICING MODEL

Pressure Pricing

Transco Zone 6				Transco Leidy Zone			
Month	n_1	n_2	n_3	Month	n_1	n_2	n_3
Apr	456	4e-5	0.0	Apr	400	3e-5	0.0
Jul	0.0	307	0.0	Jul	0.0	0.0003	0.0
Oct	415	0.0002	0.0	Oct	0.0	7e-5	0.0

Demand Pricing

Transco Zone 6 Apr				Transco Leidy Zone Apr			
Stress	m_1	m_2	m_3	Stress	m_1	m_2	m_3
1.0	0.0	465	0.1	1.0	0.0	517	0.0
6.25	0.0	513	0.2	6.25	0.0	516	0.0
9.0	0.0	505	0.07	9.0	0.0	515	0.0
Transco Zone 6 Jul				Transco Leidy Zone Jul			
1.0	0.0	477	0.4	1.0	0.0	741	0.01
6.25	0.0	609	0.8	6.25	0.0	755	0.09
9.0	0.0	760	0.1	9.0	0.0	1001	0.004
Transco Zone 6 Oct				Transco Leidy Zone Oct			
1.0	0.0	468	0.3	1.0	0.0	756	0.02
6.25	0.0	516	0.2	6.25	0.0	759	0.03
9.0	0.0	547	0.2	9.0	0.0	760	0.03

E. Alternate Pricing Models

The pricing model used in the earlier analysis was defined by the parameters in Table I, which were determined based on analysis of market data from January 2014 (the month of the Polar Vortex). In this section, we consider different parameterizations of the pricing model, which we determine empirically based on market data from April, July, and October 2014. These results show how planning for less stressed conditions leads to different solutions and also demonstrates how the pricing model can be changed in the CEGE formulation (as long as it is convex). The coefficients for the alternate parameterizations of the gas pricing model are found in Table VIII. The cost and design properties of the CEGE solutions under these alternate gas pricing parameterizations are found in Table VII. Higher temperatures in April, July, and October implied less demand for natural gas for space conditioning, and we thus observe a much lower price sensitivity. With price spikes less of an economic driver, we observe a smaller number of expansions and lower total cost of operations as compared to the results in Tables II - IV. This observation indicates that planning based on "normal" operations will underestimate infrastructure investments that are needed for extreme stress cases. The quality of the solutions found in a 12 hour limit are similar to those from the January 2014 gas pricing model, providing evidence that the computation properties do not depend heavily on the particular parameterization from January 2014.

V. CONCLUSION

We have developed and demonstrated a computationally tractable framework for modeling expansion planning decisions in nonlinear natural gas and electric power transmission systems (Combined Gas-Electric Expansion, or CEGE) that can identify cost-minimizing network expansions made for reliability reasons and expansions made for economic reasons. Our modeling framework also uses a data-driven approach to endogenizing the impacts of network expansion on natural gas and electric power operational costs.

We illustrate the CEGE model on a new joint gas-grid test system under varying demand scenarios for natural gas and electric power. Our simulation results suggest that, when demand increases by moderate amounts (1.25 or 1.3) in the electric power grid, for example) the natural gas cost impact is minimal and any network expansions can be attributed to the need to maintain sufficient delivery capacity to high-demand areas. At higher levels of demand growth, a mix of reliability-driven and economic investments emerge. We also find that the decisions to build gas or electric infrastructure to serve higher electricity demand are interchangeable, and whether it is cheaper to move electricity or move fuel over longer distances varies by location and natural gas price sensitivity.

The primary contributions of the present paper are the development and illustration of a computable CEGE model with endogenous commodity price formation, and the introduction of a new gas-grid test system that serves as a platform for computational CEGE experiments. In the present paper, we have chosen to provide detailed results for a set of experiments to provide information on the computational performance of our CEGE model as well as to articulate broad insights from a type of planning scenario for which our modeling framework may be particularly well suited.

Future work involves incorporating gas generation expansion scenarios into the CEGE model (such as some types of scenarios outlined in [2]); and conducting security-constrained joint planning for natural gas and electric power systems.

ACKNOWLEDGMENT

The authors acknowledge support from the US National Science Foundation under CMMI-1638331.

REFERENCES

[1] EPIC, "Gas-electric interface study," Eastern Interconnect Planning Collaborative, Tech. Rep., 2014. [Online]. Available: http://www.eipconline.com/gas-electric.html

[2] PJM, "PJM's evolving resource mix and system reliability," PJM Interconnection, Tech. Rep., March 2017.

[3] NERC, "Special Reliability Assessment: Accommodating an Increasing Dependence on Natural Gas for Electric Power," PLM Interconnection, Tech. Rep., May 2013.

[4] PLM Interconnection, "Analysis of Operational Events and Market Impacts During the January 2014 Cold Weather Events," PLM Interconnection, Tech. Rep., 2014.

[5] R. D. Tabors and S. Adamson, "Measurement of energy market inefficiencies in the coordination of natural gas & power," in *System Sciences (HICSS), 2014 47th Hawaii International Conference on*. IEEE, 2014, pp. 2335–2343.

[6] J. Zheng, Q. Wu, and Z. Jing, "Coordinated scheduling strategy to optimize conflicting benefits for daily operation of integrated electricity and gas networks," *Applied Energy*, vol. 192, pp. 370–381, 2017.

[7] C. Unsihuay-Vila, J. Marangon-Lima, A. Z. de Souza, I. J. Perez-Arriaga, and P. P. Balestrassi, "A model to long-term, multiarea, multistage, and integrated expansion planning of electricity and natural gas systems," *IEEE Transactions on Power Systems*, vol. 25, no. 2, pp. 1154–1168, 2010.

[8] A. Nobakht, M. Javadi, Z. Manoochehri, and S. Heidari, "Simultaneous generation expansion planning and natural gas expansion planning," *ACEEE International Journal on Control System and Instrumentation*, vol. 2, no. 1, pp. 33–38, 2011.

[9] G. Peters, "Gas and electric infrastructure interdependency analysis," Technical report prepared for the Midwest Independent Transmission System Operator (MISO), dba EnVision Energy Solutions, USA, Tech. Rep., 2012.

[10] R. Rubio-Barros, D. Ojeda-Esteybar, O. Año, and A. Vargas, "Combined operational planning of natural gas and electric power systems: State of the art," *Chapter 12, Natural Gas, edited by Primoz Potocnik*, pp. 271–288, ISBN: 978-953-307-112-1, InTech 2010.

[11] ——, "Integrated natural gas and electricity market: A survey of the state of the art in operation planning and market issues," *2008 IEEE/PES, Transmission and Distribution Conference and Exposition: Latin America, Bogota, Colombia*, pp. 1–8, 2008.

[12] M. Chaudry, N. Jenkins, M. Qadrdan, and J. Wu, "Combined gas and electricity network expansion planning," *Applied Energy*, vol. 113, pp. 1171–1187, 2014.

[13] J. Qiu, Z. Y. Dong, J. H. Zhao, K. Meng, Y. Zheng, and D. J. Hill, "Low carbon oriented expansion planning of integrated gas and power systems," *IEEE Transactions on Power Systems*, vol. 30, no. 2, pp. 1035–1046, 2015.

[14] X. Zhang, M. Shahidehpour, A. S. Alabdulwahab, and A. Abusorrah, "Security-constrained co-optimization planning of electricity and natural gas transportation infrastructures," *IEEE Transactions on Power Systems*, vol. 30, no. 6, pp. 2984–2993, 2015.

[15] Y. Hu, Z. Bie, T. Ding, and Y. Lin, "An NSGA-II based multi-objective optimization for combined gas and electricity network expansion planning," *Applied Energy*, vol. 167, pp. 280–293, 2016.

[16] C. Borraz-Sánchez, R. Bent, S. Backhaus, S. Blumsack, H. Hijazi, and P. van Hentenryck, "Convex optimization for joint expansion planning of natural gas and power systems," in *In: Proceedings of the 49th Hawaii International Conference on System Sciences (HICSS49)*, 2016, pp. Kauai, HI, January 4–8.

[17] C. Borraz-Sánchez, R. Bent, P. van Hentenryck, S. Blumsack, and H. Hijazi, "Elasticity model for joint gas-grid expansion planning optimization," in *In: Proceedings of the 47th Annual Conference, Symposium on Power Systems. Pipeline Simulation Interest Group (PSIG-1610)*, 2016, pp. Fairmont Waterfront, Vancouver, BC, Canada, May 10–13.

[18] C. Shao, M. Shahidehpour, X. Wang, X. Wang, and B. Wang, "Integrated planning of electricity and natural gas transportation systems for enhancing the power grid resilience," *IEEE Transactions on Power Systems*, 2017.

[19] C. Unsihuay-Vila, J. Marangon-Lima, and A. Zambroni de Souza, "Modeling the integrated natural gas and electricity optimal power flow," in *Proceedings 2007 IEEE Power Engineering Society (PES) General Meeting*. IEEE, 2007, pp. 24–28.

[20] S. An, Q. Li, and T. Gedra, "Natural gas and electricity optimal power flow," in *Transmission and Distribution Conference and Exposition, IEEE PES*, vol. 1, 2003, pp. 138–143.

[21] M. Chaudry, N. Jenkins, and G. Strbac, "Multi-time period gas and electricity network optimization," *Electric Power Systems Research*, vol. 78, pp. 1265–1279, 2008.

[22] C. Correa-Posada and P. Sánchez-Martín, "Security-constrained optimal power and natural-gas flow," *IEEE Transactions on Power Systems*, vol. 29, no. 4, pp. 1780–1787, 2014.

[23] M. Damavandi, I. Kiaei, M. Sheikh-El-Eslami, and H. Seifi, "New approach to gas network modeling in unit commitment," *Energy*, vol. 36, pp. 6243–6250, 2011.

[24] C. Liu, M. Shahidehpour, Y. Fu, and Z. Li, "Security-constrained unit commitment with natural gas transmission constraints," *IEEE Transactions on Power Systems*, vol. 24, no. 3, pp. 1523–1536, 2009.

[25] B. Erdener, K. Pambour, R. Lavin, and B. Dengiz, "An integrated simulation model for analysing electricity and gas systems," *Electrical Power and Energy Systems*, vol. 61, pp. 410–420, 2014.

[26] T. Leung, "Coupled natural gas and electric power systems," PhD thesis, Massachusetts Institute of Technology, Massachusetts, USA, 2015.

[27] E. Allen, J. Lang, and M. Ilić, "A combined equivalenced-electric, economic, and market representation of the northeastern power coordinating council U.S. electric power system," *IEEE Transactions on Power Systems*, vol. 23, no. 3, pp. 896–907, 2008.

[28] A. Newcomer, S. Blumsack, J. Apt, L. Lave, and M. Morgan, "The short run economic and environmental effects of a carbon tax on U.S. electric generation," *Env. Sci. Tech.*, vol. 42, pp. 3139–3144, 2008.

[29] C. Borraz-Sánchez, R. Bent, S. Backhaus, H. Hijazi, and P. van Hentenryck, "Convex relaxations for gas expansion planning," *INFORMS Journal on Computing*, vol. 28, no. 4, pp. 645–656, 2016.

[30] G. McCormick, "Computability of global solutions to factorable nonconvex programs, part i: convex underestimating problems," *Mathematical Programming*, vol. 10, pp. 147–175, 1976.

[31] H. Hijazi, C. Coffrin, and P. van Hentenryck, "Convex Quadratic Relaxations for Mixed-Integer Nonlinear Programs in Power Systems," *Mathematical Programming Computation*, pp. 1–47, 2016.

[32] S. Binato, M. V. F. Pereira, and S. Granville, "A new Benders decomposition approach to solve power transmission network design problems," *IEEE Transactions on Power Systems*, vol. 16, no. 2, pp. 235–240, 2001.

[33] D. K. Molzahn, C. Josz, I. A. Hiskens, and P. Panciatici, "A Laplacian-based approach for finding near globally optimal solutions to OPF problems," *IEEE Transactions on Power Systems*, vol. 32, no. 1, pp. 305–315, Jan 2017.

[34] EPA, "Emissions and generation resource inegrated database," Environmental Protection Agency, Tech. Rep., 2015. [Online]. Available: https://www.epa.gov/energy/emissions-generation-resource-integrated-database-egrid

[35] R. Pletka, J. Khangura, A. Rawlines, E. Waldren, and D. Wilson, "Capital Costs for Transmission and Substations," Western Electricity Coordinating Council, Tech. Rep., 2014.

[36] D. De Wolf and Y. Smeers, "Optimal dimensioning of pipe networks with application to gas transmission networks," *Operations Research*, vol. 44, no. 4, pp. 596–608, July-August 1996.

[37] T. Grant, D. Morgan, and K. Gerdes, "Carbon Dioxide Transport and Storage Costs in NETL Studies," Tech. Rep., 2014.

[38] W. Katzenstein and J. Apt, "Air emissions due to wind and solar power," *Environmental Science and Technology*, vol. 43, no. 2, pp. 253–258, 2009.

[39] J. A. Bergerson and L. B. Lave, "Should we transport coal, gas, or electricity: Cost, efficiency, and environmental implications," 2005.